

Research Article

Synthesis and Characterization of Nanoporous Monetite Which Can Be Applicable for Drug Carrier

Esmael Salimi and Jafar Javadpour

Faculty of Material Science and Engineering, Iran University of Science and Technology, Narmak, Tehran 16846, Iran

Correspondence should be addressed to Esmael Salimi, small_salim2005@yahoo.com

Received 22 May 2012; Accepted 18 October 2012

Academic Editor: Jun Liu

Copyright © 2012 E. Salimi and J. Javadpour. This is an open access article distributed under the Creative Commons Attribution License, which permits unrestricted use, distribution, and reproduction in any medium, provided the original work is properly cited.

Wormhole-like mesostructured monetite was successfully synthesized using cetyltrimethylammonium bromide ($C_{19}H_{42}BrN$, CTAB), as a porosity agent. X-ray techniques and FTIR reveal that the crystalline grains consist of highly crystalline pure monetite phase. Monetite rods with diameter around 20–40 nm and length in the range of 50–200 nm were confirmed by FESEM and TEM. Based on N_2 adsorption-desorption isotherms investigation, surface area increased up to $31.5 \text{ m}^2/\text{g}$ due to the removal of surfactant after calcinations at 400°C . The results indicate that CTAB can not only affect monetite crystallization but also change particles morphology from plate shape to rod-like.

1. Introduction

Monetite's potential as a biomaterial has recently been highlighted by a series of *in vitro*, animal and human studies in which monetite-based biomaterials have shown promising results as bone substitutes [1–3].

Monetite has a higher solubility than octacalcium phosphate, tricalcium phosphate, and calcium hydroxyapatite in aqueous solutions at the physiological pH and is considered to exhibit a high *in vivo* resorbability in comparison to the apatitic cements [3]. This high solubility has been the main stimulus for the current study.

Introduction of nano-sized pores in these materials can not only significantly enhance the total surface area but also promote adsorption of biomolecules and drugs onto the surface of the particles. It can also increase their solubility and resorbability to the high levels [4]. Since the formation of silicate-based mesoporous structure was reported in 1992 [5], it has become one of the most active research area of material science [6–8]. So far, monetite particles have been synthesized via different processing routes [9, 10]. To our best knowledge, the synthesis of mesoporous monetite has been seldom reported in the literature. In this study, we attempt to achieve the direct crystallization of mesoporous

monetite by chemical precipitation method using CTAB as a structure directing agent.

2. Experimental

2.1. Materials and Procedure. Calcium chloride (CaCl_2 , Merck Co) and diammonium hydrogen phosphate [KH_2PO_4 , Merck Co] as the Ca and P sources and CTAB as surfactant were used to synthesize nanoporous monetite powders in this study.

In a successful synthesis run to yield only single-phase CaHPO_4 , 4.075 g potassium dihydrogen phosphate [KH_2PO_4] and 5 g CTAB were dissolved in 50 mL de-ionized water at room temperature with stirring for 1 hr. Subsequently, 5.55 g CaCl_2 in 50 mL de-ionized water was added dropwise to the solution mixture, yielding a milky suspension, which was refluxed at 120°C for 24 h.

The pH value was adjusted to $\text{pH} = 4\text{--}5$. The suspension was then transferred into a 100 mL PTFE-lined autoclave and heated at $90\text{--}150^\circ\text{C}$ in an oven for a specified time. The precipitate was filtered and washed several times with distilled water to remove contaminated ions and surfactant. Then, it was dried at 100°C for 24 h. Calcination of powder was carried out at different temperature (up to 550°C).

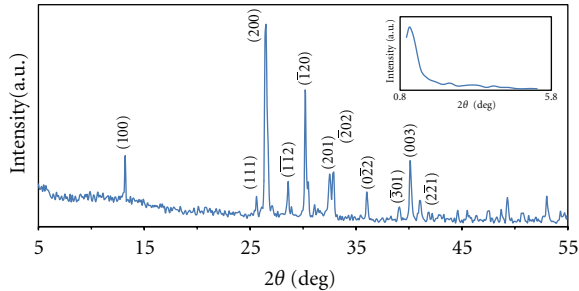


FIGURE 1: WAXRD and LAXRD (inset) pattern of as-dried nanoporous monetite.

2.2. Characterization. The X-ray powder diffraction patterns were recorded on a Philips 1830 diffractometer using $\text{Cu-K}\alpha$ radiation at 40 kV and 40 mA. Nitrogen adsorption-desorption isotherms of the synthesized samples were measured at 77 K on Micromeritics model ASAP 2010 sorptometer to determine pore-size distribution and surface area of the samples. Energy dispersive X-ray (EDX) element analysis was carried out on the JEOL 6300F scanning microscope. The morphology of the powders was examined by scanning (SEM, JEOL 6300F) and transmission (TEM, Philips CM120) electron microscopy. The Fourier transform infrared spectra of samples were measured on a DIGILAB FTS 7000 instrument under attenuated total reflection (ATR) mode using a diamond module. TGA (Perkin-Elmer 7 series thermal analysis system) was performed at $10^\circ\text{C}/\text{min}$ from room temperature to 800°C to determine the thermal behavior of the synthesized monetite.

3. Results and Discussion

Figure 1 shows the XRD patterns of the as-dried and calcined monetite. WAXRD patterns (Figure 1) of the nanoparticles consist of narrow peaks with d spacing consistent with well-ordered crystalline monetite. (JCPDS 71-1759). The chemical reaction for the formation of monetite can be simplified as $\text{Ca}^{+2} + \text{H}_2\text{PO}_4^- = \text{CaHPO}_4 + \text{H}^+$.

The peaks within small angle range (2θ 1– 10°) provide information on the arrangement presented by porous structure [11].

For LAXRD (Figure 1 inset), the pattern of the as-dried sample shows a single intense diffraction peak at 2θ value of 1.114° ($d = 7.92\text{ nm}$). The single peak suggested the presence of disordered mesoporous structure inside the sample, such as worm-like mesopores [11, 12].

Figures 2(a) and 2(b) show the FTIR spectra of calcium phosphate before and after calcinations. Figure 2(a) shows only the characteristic IR bonds of monetite [13–18].

The wavenumbers and corresponding assignment are represented in Table 1.

The adsorption bands at 2921 cm^{-1} , 1637 cm^{-1} , and 1400 cm^{-1} are characteristic peaks for $\mu(\text{C-H})$, $\delta(\text{N-H})$, and $\delta(\text{C-H})$, respectively [13, 18], that reveal the presence of surfactant in monetite structure. These results are in accordance with the XRD (Figure 1) description above,

TABLE 1: The wavenumbers and corresponding assignments of monetite.

IR monetite wavenumbers (cm^{-1})	Assignments
2921	C–H stretching [19]
2852	
3461	O–H stretching of residual free water [14]
902	P–O(H) stretching [13, 19]
1064	P–O stretching [14, 19]
1130	
1637	H–O–H bending and rotation of residual free water [14]
1400	P–O–H in plane (bending) [14]
530	O–P–O(H) bending mode [14]
583	
1419	Carbonate (from atmosphere) [15]

demonstrating that single-phase and highly crystalline monetite can be obtained with the aid of surfactant as a template, while Figure 2(b) reveals the adsorption bands for calcium pyrophosphate polycrystalline.

The bands at 530 cm^{-1} [19], 1031 cm^{-1} [18, 19], 1139 cm^{-1} [20], 563 cm^{-1} [20], and 1074 cm^{-1} [20] are ascribed to PO_4^{3-} ions, at 1556 cm^{-1} to CO_3^{2-} ions [18]. A very sharp and intense band appears around $\sim 721\text{ cm}^{-1}$ due to $\text{P}_2\text{O}_7^{4-}$ showing the presence of calcium pyrophosphate ($\text{Ca}_2\text{P}_2\text{O}_7$) [20], and the band at $\sim 3430\text{ cm}^{-1}$ is assigned to the bending mode of the OH^{-1} vibration [13]. The FTIR spectrum shows no adsorption band related to organic molecules. So, it can be concluded that, there is no residual surfactant in the structure after calcinations.

Adsorption-desorption isotherms and pore size distributions of mesoporous monetite calcined at different temperatures are shown in Figure 3. Appropriate calcination temperatures concluded from thermogravimetric analysis. Samples calcined at 200°C , 400°C , and 470°C exhibit a mesoporous materials type IV curve with a hysteresis loop. The BET surface area is calculated to be $31.3\text{ m}^2/\text{g}$, $31.5\text{ m}^2/\text{g}$, and $28.8\text{ m}^2/\text{g}$ for samples calcined at 200°C , 400°C , and 470°C , respectively.

The low specific is attributed to the formation of mesostructure with thick walls (Figure 4(d)), though the pore volume is high. After calcination at high temperature ($>500^\circ\text{C}$), due to the conversion of monetite to calcium pyrophosphate (Figure 1), the porous structure is collapsed and the specific surface area decreased to $5.22\text{ m}^2/\text{g}$ as indicated in Figure 3(d). The pore volume was evaluated as $0.99\text{ cm}^3/\text{g}$, $0.98\text{ cm}^3/\text{g}$, and $0.3\text{ cm}^3/\text{g}$ for samples calcined at 200°C , 400°C , and 470°C , respectively.

Precipitation of calcium phosphate without template is successfully performed by mixing KH_2PO_4 (3 M) and NaOH (1 M) with CaCl_2 (5 M) with a pH sufficient to obtain monetite.

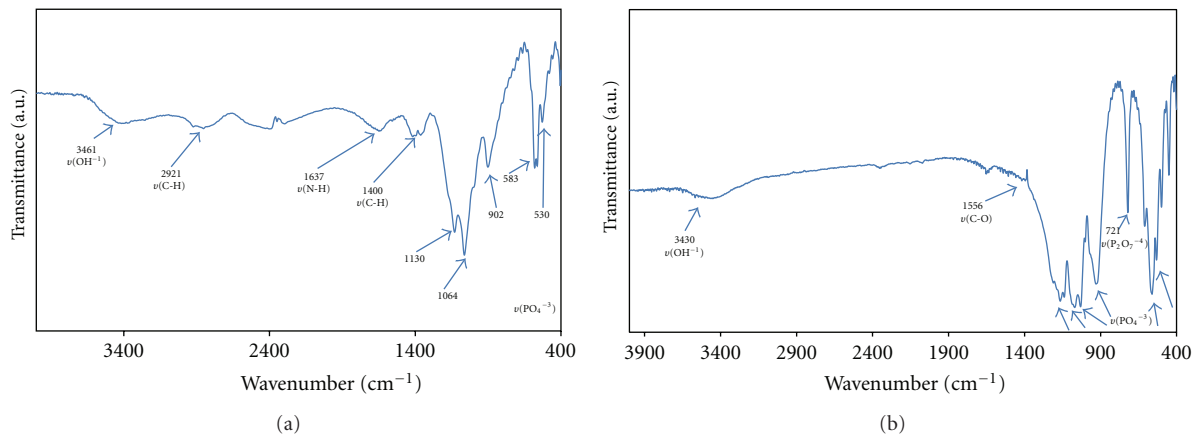


FIGURE 2: FTIR spectrum of (a) nanoporous monetite and (b) calcium pyrophosphate prepared after calcinations of nanoporous monetite at 550°C.

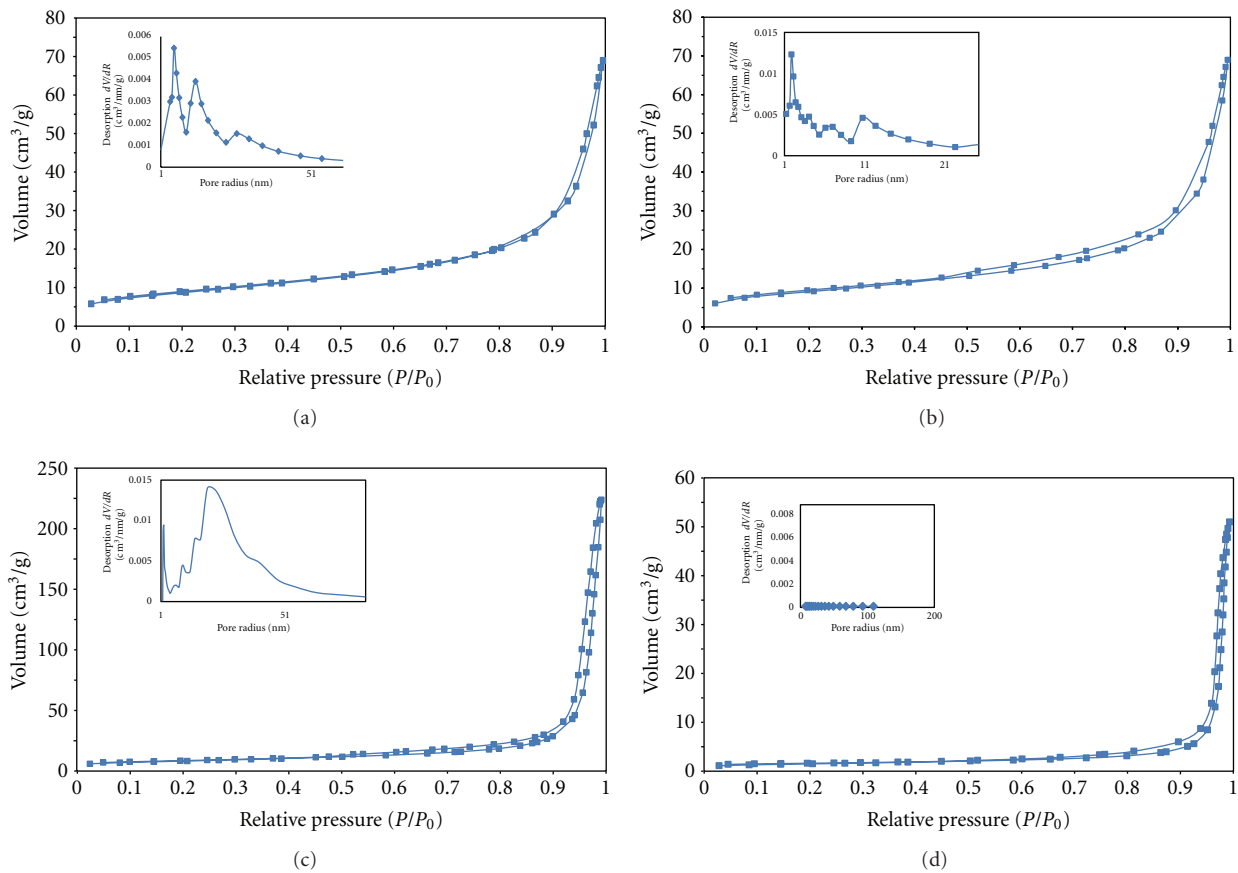


FIGURE 3: Nitrogen adsorption-desorption isotherms of nanoporous monetite after calcination at (a) 200°C, (b) 400°C, (c) 470°C, and (d) 550°C.

It can be seen that the monetite prepared without CTAB (Figures 4(a) and 4(b)) is almost agglomerated plate-shape, with lateral sizes of 2–10 μm and thickness of 1–3 μm .

The TEM micrograph of the prepared nanoporous monetite sample (Figure 4(c)) shows that the synthesized monetite is fairly dispersed nanorods of diameter 20–40 nm and in the length range of 50–200 nm. It is clear that

the morphology and size of monetite can be controlled effectively by using CTAB.

EDX analysis indicated a Ca : P ratio of approximately 1, characteristic of monetite. A bright cylindrical restrict (not very obvious) can be seen in the center of rods (Figure 4(d)). It seems that it is a hollow space, originated due to the removal of surfactant. The rod-like micelles formed during

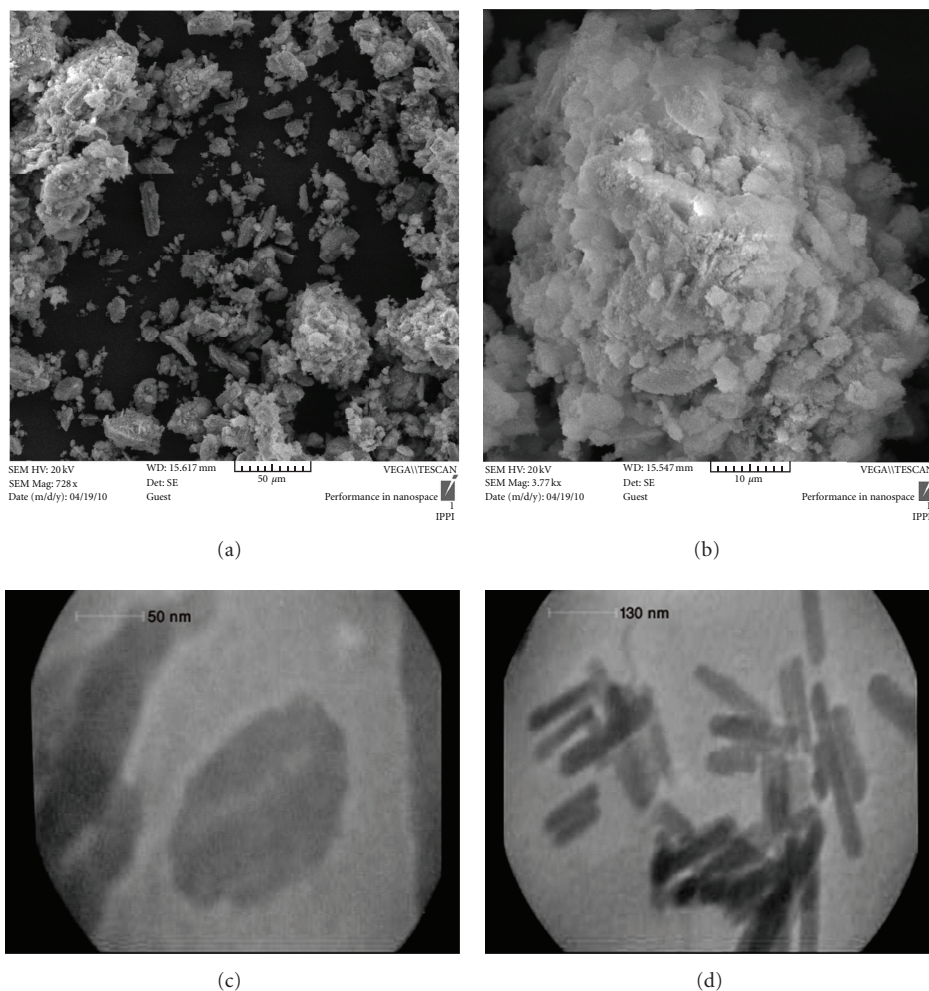


FIGURE 4: (a) and (b) SEM micrographs of monetite prepared without surfactant; (c) and (d) TEM micrograph of nanoporous monetite.

the synthesis and served as templates. The micelles, not only provide nucleation sites for target materials induced the orientational growth of the monetite particles, but also create nanopores in the structure.

4. Conclusions

Monetite particles with mesoporous structure and controlled morphology were successfully synthesized using CTAB as cationic surfactant. A strong association between the CaHPO_4 and surfactant molecules throughout the development of the crystal could be responsible for the formation of well-crystallized monetite with rod-like morphology. However, the mesostructured phase was unstable at higher temperature because of the transformation of monetite to calcium pyrophosphate.

Acknowledgment

Research council of Iran University of Science and Technology (IUST, Iran) is appreciated for the financial support.

References

- [1] U. Gbureck, T. Hölzel, U. Klammert, K. Würzler, F. A. Müller, and J. E. Barralet, "Resorbable dicalcium phosphate bone substitutes prepared by 3D powder printing," *Advanced Functional Materials*, vol. 17, no. 18, pp. 3940–3945, 2007.
- [2] P. Habibovic, U. Gbureck, C. J. Doillon, D. C. Bassett, C. A. van Blitterswijk, and J. E. Barralet, "Osteoconduction and osteoinduction of low-temperature 3D printed bioceramic implants," *Biomaterials*, vol. 29, no. 7, pp. 944–953, 2008.
- [3] F. Tamimi, J. Torres, D. Bassett, J. Barralet, and E. L. Cabarcos, "Resorption of monetite granules in alveolar bone defects in human patients," *Biomaterials*, vol. 31, no. 10, pp. 2762–2769, 2010.
- [4] H. C. Shum, A. Bandyopadhyay, S. Bose, and D. A. Weitz, "Double emulsion droplets as microreactors for synthesis of mesoporous hydroxyapatite," *Chemistry of Materials*, vol. 21, no. 22, pp. 5548–5555, 2009.
- [5] C. T. Kresge, M. E. Leonowicz, W. J. Roth, J. C. Vartuli, and J. S. Beck, "Ordered mesoporous molecular sieves synthesized by a liquid-crystal template mechanism," *Nature*, vol. 359, no. 6397, pp. 710–712, 1992.
- [6] M. Anbia and S. E. Moradi, "Adsorption of naphthalene-derived compounds from water by chemically oxidized

- nanoporous carbon,” *Chemical Engineering Journal*, vol. 148, no. 2-3, pp. 452–458, 2009.
- [7] M. Anbia and A. Ghaffari, “Adsorption of phenolic compounds from aqueous solutions using carbon nanoporous adsorbent coated with polymer,” *Applied Surface Science*, vol. 255, no. 23, pp. 9487–9492, 2009.
- [8] M. Anbia and N. Mohammadi, “A nanoporous adsorbent for removal of furfural from aqueous solutions,” *Desalination*, vol. 249, no. 1, pp. 150–153, 2009.
- [9] Y. Guo, Y. Zhou, D. Jia, and H. Tang, “Fabrication and characterization of hydroxycarbonate apatite with mesoporous structure,” *Microporous and Mesoporous Materials*, vol. 118, no. 1-3, pp. 480–488, 2009.
- [10] S. Jinawath and P. Sujaridworakun, “Fabrication of porous calcium phosphates,” *Materials Science and Engineering C*, vol. 22, no. 1, pp. 41–46, 2002.
- [11] Y. F. Zhao and J. Ma, “Triblock co-polymer templating synthesis of mesostructured hydroxyapatite,” *Microporous and Mesoporous Materials*, vol. 87, no. 2, pp. 110–117, 2005.
- [12] H. Guo, F. Ye, and H. Zhang, “Tween-60 mediated synthesis of lamellar hydroxyapatite with worm-like mesopores,” *Materials Letters*, vol. 62, no. 14, pp. 2129–2132, 2008.
- [13] Q. Ruan, Y. Zhu, Y. Zeng et al., “Ultrasonic-irradiation-assisted oriented assembly of ordered monetite nanosheets stacking,” *Journal of Physical Chemistry B*, vol. 113, no. 4, pp. 1100–1106, 2009.
- [14] S. Mandel and A. C. Tas, “Brushite ($\text{CaHPO}_4 \cdot 2\text{H}_2\text{O}$) to octacalcium phosphate ($\text{Ca}_8(\text{HPO}_4)_2(\text{PO}_4)_4 \cdot 5\text{H}_2\text{O}$) transformation in DMEM solutions at 36.5°C ,” *Materials Science and Engineering C*, vol. 30, no. 2, pp. 245–254, 2010.
- [15] A. Lebugle, B. Sallek, and A. Tai Tai, “Surface modification of monetite in water at 37°C : characterisation by XPS,” *Journal of Materials Chemistry*, vol. 9, no. 10, pp. 2511–2515, 1999.
- [16] A. C. Tas, “Monetite (CaHPO_4) synthesis in ethanol at room temperature,” *Journal of the American Ceramic Society*, vol. 92, no. 12, pp. 2907–2912, 2009.
- [17] E. Fernandez, M. P. Ginebra, M. G. Boltong et al., “Kinetic study of the setting reaction of a calcium phosphate bone cement,” *Journal of Biomedical Materials Research*, vol. 32, pp. 367–374, 1996.
- [18] X. Xin-Bo, Z. Xie-Rong, Z. Chun-Li, L. Ping, and F. Yun-Bo, “Influence of hydrothermal temperature on hydroxyapatite coating transformed from monetite on HT-C/C composites by induction heating method,” *Surface and Coatings Technology*, vol. 204, no. 1-2, pp. 115–119, 2009.
- [19] P. M. SL Shanthi, M. Ashok, T. Balasubramanian, A. Riyasdeen, and M. A. Akbarsha, “Synthesis and characterization of nano-hydroxyapatite at ambient temperature using cationic surfactant,” *Materials Letters*, vol. 63, no. 24-25, pp. 2123–2125, 2009.
- [20] S. Singh, P. Bhardwaj, V. Singh, S. Aggarwal, and U. K. Mandal, “Synthesis of nanocrystalline calcium phosphate in microemulsion-effect of nature of surfactants,” *Journal of Colloid and Interface Science*, vol. 319, no. 1, pp. 322–329, 2008.

